Pharm Res (2014) 31:1325–1337
DOI 10.1007/s11095-013-1253-7

RESEARCH PAPER

The Influence of Actuator Materials and Nozzle Designs on Electrostatic Charge of Pressurised Metered Dose Inhaler (pMDI) Formulations

Yang Chen • Paul M. Young • David F. Fletcher • Hak Kim Chan • Edward Long • David Lewis • Tanya Church • Daniela Traini

Received: 9 July 2013 / Accepted: 10 November 2013 / Published online: 3 December 2013

ABSTRACT

Purpose To investigate the influence of different actuator materials and nozzle designs on the electrostatic charge properties of a series of solution metered dose inhaler (pMDI) aerosols.

Methods Actuators were manufactured with flat and cone nozzle designs using five different materials from the triboelectric series (Nylon, Polyethylene terephthalate, Polyethylene–High density, Polypropylene copolymer and Polytetrafluoroethylene). The electrostatic charge profiles of pMDI containing beclomethasone dipropionate (BDP) as model drug in HFA-134a propellant, with different concentrations of ethanol were studied. Electrostatic measurements were taken using a modified electrical low-pressure impactor (ELPI) and the deposited drug mass assayed chemically using HPLC.

Results The charge profiles of HFA 134a alone have shown strong electronegativity with all actuator materials and nozzle designs, at an average of −1531.34 pC ± 377.34. The presence of co-solvent ethanol significantly reduced the negative charge magnitude. BDP reduced the suppressing effect of ethanol on the negative charging of the propellant. For all tested formulations, the flat nozzle design showed no significant differences in net charge between different actuator materials, whereas the charge profiles of cone designs followed the triboelectric series.

Conclusion The electrostatic charging profiles from a solution pMDI containing BDP and ethanol can be significantly influenced by the actuator material, nozzle design and formulation components. Ethanol concentration appears to have the most significant impact. Furthermore, BDP interactions with ethanol and HFA have an influence on the electrostatic charge of aerosols. By choosing different combinations of actuator materials and orifice design, the fine particle fractions of formulations can be altered.

KEY WORDS electrostatics charges · metered dose inhalers · nozzle designs · triboelectric series

INTRODUCTION

It has long been speculated that electrostatic charges carried by aerosol particles can influence the deposition of inhaled aerosol particles in the lungs. Experimental studies using a hollow lung cast (1) and *in vivo* experiments with humans (2,3) and animals (4–6) with non-therapeutic compounds such as wax, dust and asbestos, have all shown a significant increase in deposition for charged particles. In addition, theoretical considerations (7–10) have revealed increased deposition for charged particles is possible under appropriate conditions.

Y. Chen • P. M. Young • D. Traini (✉)
Respiratory Technology
Woolcock Institute of Medical Research and Discipline of Pharmacology
Sydney Medical School, University of Sydney, Sydney
NSW 2037, Australia
e-mail: Daniela.traini@sydney.edu.au

D. F. Fletcher
School of Chemical and Biomolecular Engineering
University of Sydney, Sydney, NSW 2006, Australia

H. K. Chan
Advanced Drug Delivery Group, Faculty of Pharmacy (A15)
University of Sydney, Sydney, NSW 2006, Australia

E. Long
Wolfson School of Mechanical and Manufacturing Engineering
Loughborough University, Loughborough, Leicestershire LE11 3TU, UK

D. Lewis • T. Church
Chiesi Ltd, Units T1 - T3, Bath Rd. Ind. Est, Chippenham
Wiltshire SN14 0AB, UK

Electrostatic charges on aerosol particles can influence the behavior of particle deposition in the lung. Firstly, 'space charges', relating to the mutual repulsive force generated by the electron cloud surrounding each of the charged particles, can lead to increased deposition, caused by the deflection of the particles toward the airway wall (11). Secondly, image charges, where enhanced particle-wall attraction is achieved via charged particles inducing a transient charge of opposite polarity at the airway wall (11,12). In the pharmaceutical industry, electrostatic phenomena have been a topic of debate and research for many years, since they have a huge impact on formulation performance, where powder and small particles are used during bulk material blending, tableting/capsule manufacture and filling process (13–16).

The impact of charge on the delivered dose and aerosol performance of inhalation based drug formulations is very important and depends on many variables, including their formulation and manufacture, dosing reproducibility and deposition behavior within the respiratory tract and/or spacer devices (12,13,17). Therapeutic aerosols generated by nebulizers (18), pressurised metered dose inhalers (pMDIs) (19,20) and dry powder inhalers (DPIs) (21–25) are known to be charged (26). The mechanism involved in the charging process for pharmaceutical aerosols are contact and/or friction charging, which is normally referred as triboelectrification.

Pressurised metered dose inhalers are pharmaceutical delivery systems containing a drug, either suspended or solubilised using co-solvents, in a hydro-fluoro-alkane (HFA) propellant with or without stabilising excipients (27). Upon actuation, the canister is depressed and the metering chamber containing a specific volume of formulation mixture is released from the valve to the expansion chamber (28). Once exposed to atmospheric pressure, the pressurised liquid propellant experiences a high pressure gradient and rapidly changes from a liquid to vapour containing evaporating droplets. This process if called flash evaporation (29). Subsequently, due to the high vapour pressure of the propellant and rapid expansion after actuation, the droplets in the atomised cloud continues to evaporate until the non-volatile components solidify as fine particles (30). This phase transition represents the driving force necessary to aerosolise the drug and determines its lung deposition.

Drug deposition of pMDIs can be influenced by many factors, such as particle/droplet size (31,32), plume exit velocity and geometry (33), inspiratory flow rate (34) and electrostatic charge of the particle/droplets and device/actuator components (35,36). While the majority of these factors have all been investigated, various aspects related to the electrostatic charging effect of pMDIs have not been explored in depth.

Researchers have investigated variables including ex-valve effects, for example the use of spacers (37,38) and in-formulation effects, such as the impact of the presence of moisture (39) on pMDI aerosol electrostatics. Other variables such as the material used for the actuator and nozzle design that could have a significant impact on the charge and consequently on the performance of the aerosols, have not been investigated fully. In 2003 Berry *et al*. investigated the influence of the metering chamber volume and actuator design (orifice diameters of 0.5 mm and 1 mm) of pMDIs (40) and concluded that while the valve-metering chamber volume (25 versus 63 μL) did not appear to have a major effect on the aerodynamic or droplet size, the actuator design and orifice size had instead a significant effect. Also, Smyth *et al*., in 2006, investigated the effect of sump depth and actuator orifice length and size (41,42). They also found that both parameters influenced the aerosol spray pattern significantly. However, very little can be found in the literature regarding the effect of electrostatic charge accumulation and decay on the surface of pharmaceutical polymer materials used in pMDI actuators. Carter *et al*. presented a very brief study in 1998 where it was demonstrated that different polymer discs used for actuator material manufacture had different charge accumulation and decay properties (43).

Various materials have a tendency of either giving up electrons and becoming positive (+) or attracting electrons and becoming negative (−) in charge. These differences in charging properties between materials are based on their work function and can be expressed as a triboelectric series, shown in Fig. 1 (44,45). The position of the material within the two polarities of the triboelectric series gives a theoretical prediction of the net surface charge that results from the contact with another material. Studies conducted by both Saleh and Ndama in 2011 demonstrated that, due to triboelectrification, different pipe materials on a pneumatic conveyor transferred specific charges to powders like sugar, PVC and glass, e.g. PTFE pipe gave positive charged particles and nylon material resulted in particles with opposite polarity (46,47). These results reflected the charging profile for the material predicted by the triboelectric series (e.g., PTFE is predicted to be negatively charged resulting in positive charged particles). Moreover, contact and separation of the same material also generates net charges. This is not explained by triboelectrification since electron transfer between materials can also be influenced by variables such as

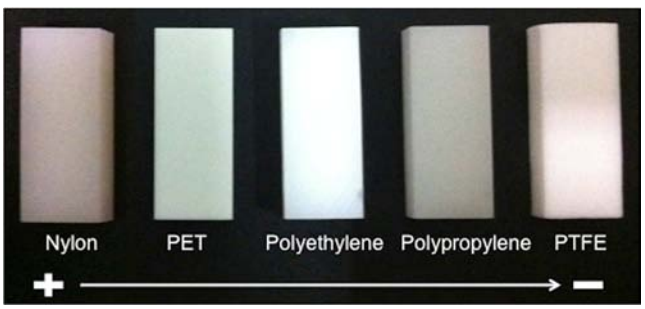

Fig. 1 Thermoplastic materials used for actuator manufacture and their respective charging properties in the triboelectric series.

material impurities, contact area, velocity, particle size, surface roughness and/or humidity (45,48,49).

Generally, the material used in pMDIs actuators is polypropylene. To the author's knowledge, no studies have been performed studying the influence of actuator material and nozzle orifice design on the electrostatic change of aerosols generated from solution pMDIs. Therefore, the aim of this study is to investigate the electrostatic charging properties of a model solution-based pMDI containing beclomethasone dipropionate as the model drug and ethanol as co-solvent, using different actuator materials selected from the triboelectric series. Two different nozzle orifice designs are also investigated.

MATERIALS AND METHODS

Materials

The pMDI actuator blocks were manufactured using five different thermoplastic materials, selected according the triboelectric series, from positive to negative charges (Fig. 1). Specifically: Nylon (Polyamid 6), Polyethylene terephthalate (PET), Polyethylene–High density (PE) and Polytetrafluoroethylene (PTFE) materials were obtained from Ensinger GmbH (Nufringen, Germany). Polypropylene copolymer (PP, polypropylene) was obtained from Doeflex Compounding Ltd (Wiltshire, UK) and used as supplied to prepare the actuator blocks.

Standard aluminium pMDI canisters C128P (ID214, Batch 1002043–3, 18 ml brim capacity) were supplied by Presspart Manufacturing Ltd (Lancashire, UK) and equipped with 50 μl metered valves (ID201, batch BK0313029) consisting of an aluminium ferrule, polyester/nylon body, EPDM/NBR/Butyl seats and gasket, acetal/polyester metering chamber and stainless steel spring from Bespak Europe Ltd (Norfolk, UK). 1,1,1,2-Tetrafluoroethane (HFA 134a) was obtained from INEOS Fluor Americas LLC (LA, USA). The active pharmaceutical ingredient (API): Beclomethasone dipropionate (BDP) was kindly supplied by Chiesi Farmaceutici S.p.A (Parma, Italy). Water used throughout the study was prepared by reverse osmosis (Milli-Q, Sydney, Australia). All analytical grade chemicals were obtained from Sigma-Aldrich Pty Ltd (Castle Hill, Australia).

Pressurised Dose Inhaler Formulation Manufacture

Four pMDI formulation compositions were prepared according to Table I. The weight of ethanol or ethanol containing solubilized BDP was calculated according to the desired percentage and accurately weighed into the aluminium pMDI canister. Each canister was fitted with a 50 μl metering valve and immediately crimped and pressure filled using a Pamasol Laboratory plant P2016 (Pamasol Willi Maäden AG, Pfaffikon, SZ) with HFA134a. Solubility of the drug components was confirmed visually using glass canisters (Saint Gobain plc.). All canisters were stored at ambient temperature for 24 h prior to testing.

Table I Pressurised Metered Dose Inhaler (pMDI) Formulation Composition

Formulation name*	Targeted Dose (μg)	BDP (% w/w)	Ethanol (% w/w)	HFA 134a (% w/w)
HFA	NA	NA	0	100
HFA-1%	NA	NA	1	99
HFA-15%	NA	NA	15	85
BDP	50	0.1	14.9	85

* HFA: HFA 134a used throughout the formulation; BDP: beclomethasone dipropionate

Actuator Block Design and Manufacture

Actuator nozzles (actuator blocks), with a nominal atomization orifice diameter of 0.3 mm, were manufactured from the actuator blocks of previously selected materials.

Two types of actuator nozzle were used in this study, one with a flat profile at the exit of the atomisation orifice and one with a cone profile (shown in Fig. 2a and b). These nozzles were designed in *Siemens NX* software and manufactured using high-speed-steel cutting tools. The components were water cooled during manufacture in order to maintain their dimensional accuracy, with the exception of the Nylon actuators, which were pre-chilled and air-cooled. This different approach was taken for the Nylon components because of Nylon's high level of water-absorption, which would have affected its volume during manufacture. Orifice diameters were checked using a spatially calibrated microscope and *MediaCybernetics* Image-Pro software; this measurement demonstrated that dimensional accuracy to within ±0.01 mm was achieved.

Prior to use, all actuator blocks were washed with water and ethanol in a sonication bath followed by air-drying before further use. Custom-made adaptors (Fig. 2c) for housing the actuator blocks and allowing connection to the United States Pharmacopeia (USP) induction port were designed using computer aided design (ANSYS DesignModeler release 13, ANSYS Inc, PA, USA) and built in acrylonitrile butadiene styrene (ABS) using a 3D printer (Dimension Elite, MN, USA).

Surface Energy Measurement of Actuator Blocks

The dispersive and polar contribution to the surface energy of each actuator block was measured using contact angle measurements, via the sessile drop method described elsewhere

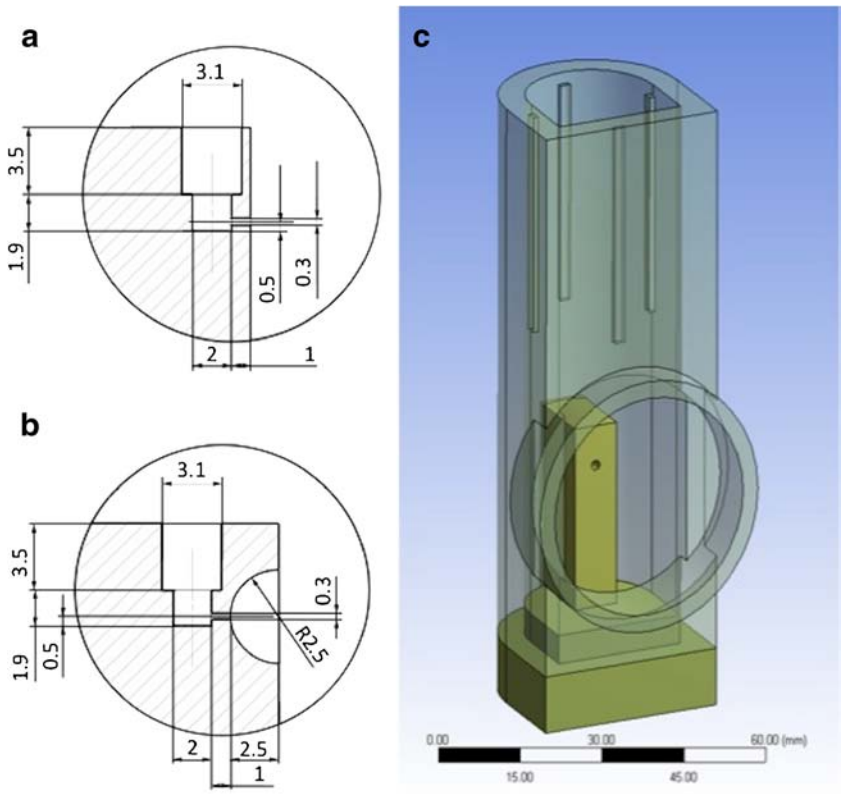

Fig. 2 Actuator nozzle designs: flat (**a**), cone (**b**), and (**c**) pMDI adaptor for the actuator blocks (**c**). Design units in mm.

(50, 51). Measurements were conducted using a NRL goniometer (Model 200-00; Ramé-Hart, Inc., Netcong, NJ) equipped with Dropimage Standard software. A microsyringe was used to deposit a fixed volume of probe solution onto the actuator block surface and advancing contact angles were measured. Three different liquids (diiodomethane, glycerol and water) with known nonpolar, acid (γ^+, electron-acceptor) and base (γ^-, electron-donor) surface tension components were used. The Young–Dupré equation was used to calculate each surface energy parameter (52).

Aerosol and Electrostatic Charge Measurements Using the ELPI

The electric low-pressure impactor (ELPI™, Dekati, Ltd. Finland) is a 13-stage impactor with an aerodynamic diameter cut-off range between 0.028 μm and 10.07 μm, at a flow rate of 30 L/min. Each impaction stage is isolated and connected to an individual digital ammeter that records current in femto amps per second (fA/s). An ELPI equipped with an USP induction port, without the corona charger, was used to measure the native electrostatic charges for the pMDI aerosols clouds (Fig. 3). Prior to analysis, the pMDI canisters were shaken thoroughly and primed to waste twice using a commercial actuator, before being fitted to the house-built adaptor unit containing the different actuator blocks with the two different nozzle designs, and connected to the ELPI via the USP Induction port and corona frame. The flow rate was set at 30 L/min using a Sogevac ® model SV25 vacuum pump

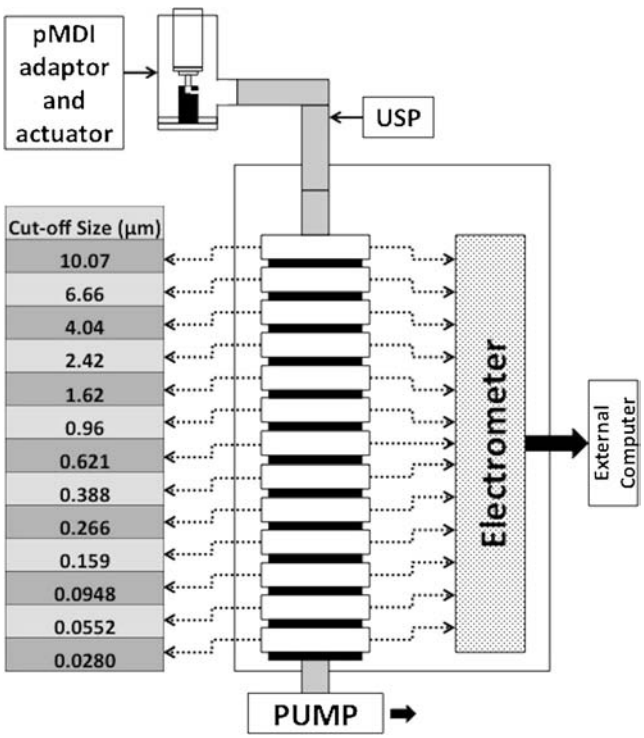

Fig. 3 ELPI set up for electrostatic measurements with aerodynamic cut-off sizes for each stage.

(Leybold, France) and calibrated using a Copley ® model 4000 flow meter (Nottingham, UK). The electrometer baseline for the ELPI was zeroed after the peak flow rate was achieved. Five single doses from each pMDI formulation were dispersed into the ELPI with a 30 s delay in between each actuation. Five actuations were chosen to minimize variation, to obtain a more reproducible charge profile and to ensure a drug deposition on the ELPI stages above the limit of detection for further chemical analysis.

During dispersion, current versus time data from each stage were collected by the electrometer and recorded by ELPI-VI 4.0 software (Dekati Ltd, Finland). Results were integrated to produce plate charge data. After all five actuations (equivalent to 250 μg total dose of BDP), the adaptor, USP induction port, corona frame and impactor stages were each washed with methanol/H_2O (80:20 v/v) rinsing solution into suitable volumetric flasks. The recovered drug samples were analysed using high performance liquid chromatography (HPLC).

No chemical analyses were performed for pMDIs containing HFA-only, HFA-1% and HFA-15% as these formulations contained no drug. In these cases, only charge data were collected and analysed. All experiments were randomized and performed in triplicate under laboratory environment conditions (temperature ~25°C and relative humidity ~40–50%).

Drug Quantification by High Performance Lliquid Chromatography (HPLC)

Chemical analysis of BDP was performed by HPLC using a Shimadzu prominence UFLC system equipped with an SPD-20A UV–Vis detector, LC-20AT solvent delivery unit, SIL-20A HT autosampler (Shimadzu Corporation, Japan) and a 3.9×150 mm Nova-Pak® C18 column (Waters Corporation, Milford Massachusetts, USA). Data were recorded at a UV Detector setting of 240 nm and integrated using Shimadzu LCSolution workstation software (Shimadzu Corporation, Japan). The mobile phase consisted of a mixture of methanol and 0.05% w/v ammonia acetate aqueous solution (68:32%, v/v). The flow rate was set at 1 mL/min with an injection volume of 100 μl. BDP standards were prepared daily in a methanol: H_2O (80:20%, v/v) rinsing solution. Linearity of BDP was obtained between 1 and 50 μg/mL (R^2=0.999) with a retention time of ~5 min.

Statistical Analysis

Electrostatic and mass deposition data for each experiment was based on the mean charge and mass per stage for three runs each, consisting of five consecutive shots. Two sample Student *t*-test (heteroscedastic) and one-way ANOVA (Unstacked) analysis were performed using the STATPlus® statistics software package (AnalystSoft Inc, VA, USA). Significant difference was based on $p<0.05$.

RESULTS AND DISCUSSION

The effects of formulation components (ethanol concentrations and drug), nozzle design and actuator materials have been investigated and the results presented below.

The Effect of Formulation Contents and Nozzle Designs on the Overall Net Charge Performance for PMDI Aerosol

The net charge for each experiment was calculated as the total charge from the 13 stages of the ELPI. The mean of three experiments for different pMDI formulations with all the different materials and both nozzle designs (flat and cone) are shown in Figs. 4, 5, 6, and 7.

Influence of HFA on Net Electrostatic Charge

In general, for the HFA only formulation the charge of the un-evaporated droplets produced negative charge profiles (average −1531.34 pC±377.34) across all stages for all materials and nozzle designs (Fig. 4). Furthermore, the value of the net negative charge was greatest for the HFA only formulation.

The chemical structure of HFA 134a contains four-fluorine atoms (CH_2FCF_3) with a high affinity for electrons via the electron withdrawing –F molecules. Although the five different materials used for the actuators had different triboelectric properties, from positive to negative, results showed that the overall electronegativity of the HFA 134a molecule, for both nozzle designs, overwhelms the contribution offered by the materials upon contact of the droplets by the aerosol plume during actuation.

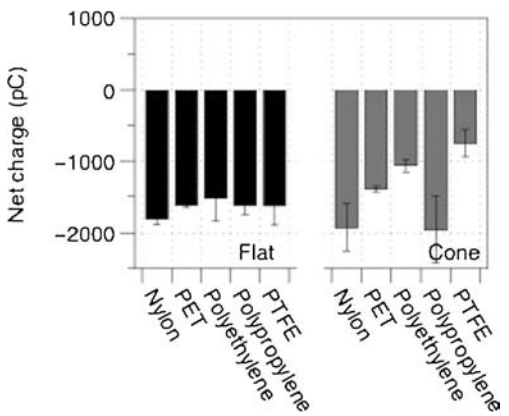

Fig. 4 Net charge for all materials and both nozzle designs (flat and cone) for the formulation containing 100% HFA, ($n=3$, pC±SD).

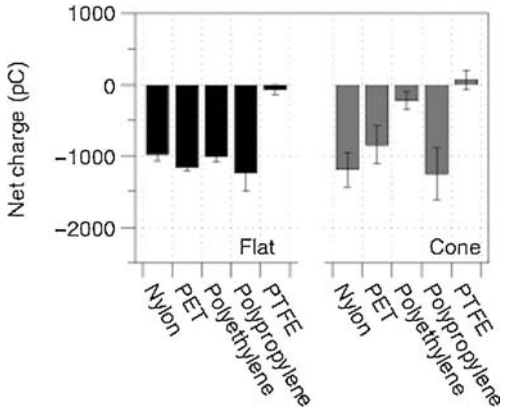

Fig. 5 Net charge for all materials and both nozzle designs (flat and cone) for the formulation containing 99% HFA and 1% w/w Ethanol, ($n = 3$, pC ± SD).

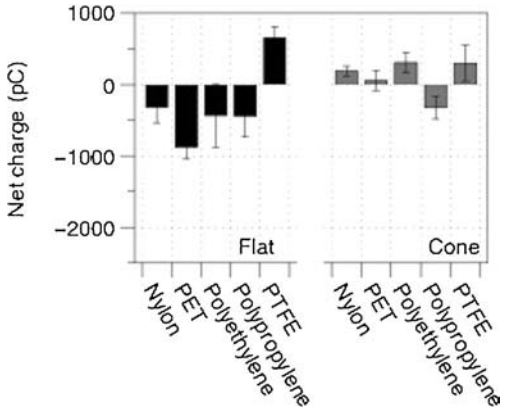

Fig. 7 Net charge for all materials and both nozzle designs (flat and cone) for the formulation containing 0.1% w/w BDP 14.9% w/w ethanol and HFA, ($n = 3$, pC ± SD).

Considering the flat nozzle design, no significant difference in charge was observe when comparing materials (One-way ANOVA, $p = 0.536$), still it produced −1500 to −2000 pC of net charge, implying that there was some charging, but most likely related to the atomization mechanism itself rather than contact charging with the actuator nozzle surface.

In comparison, the cone nozzle design showed significant differences in charge between materials, with a ranking of: PTFE < PE < PET < Nylon. Such observations suggest that the higher contact area available between the propellant and actuator material in the cone material resulted in a greater opportunity for charge exchange at the exit orifice.

In general, the rank order of charge for the cone geometries followed the triboelectric series, with the exception of Polypropylene which indicated a similar net charge to Nylon with values of: –1926.12 pC (± 327.37) and –1957.27 pC (± 464.50), respectively. It is expected that the polypropylene (PP) did not fit in the triboelectric series since it is a co-polymer. To further understand the impact of the polypropylene co-polymer on charging, the surface energy of each materials was measured and compared with the net charge data presented in Fig. 4.

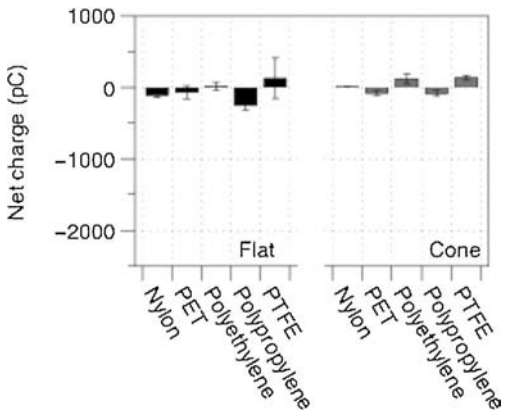

Fig. 6 Net charge for all materials and both nozzle designs (flat and cone) for the formulation containing 85% HFA and 15% w/w Ethanol, ($n = 3$, pC ± SD).

Table II shows the surface energy parameters for each actuator block, measured using contact angle goniometry. Analysis of the total surface energy indicated a rank order of Nylon > PP > PET > PE > PTFE. Based on surface energy data, the rank change in net negative charge for cone geometry follows that of the total surface energy. On the other hand, the aerosol plume passing through the cone nozzle design will have a tendency to be deflected by the outer edge of the nozzle. The sharp edge within the cone design is potentially a point of electrostatic field intensification, and specifically with HFA 134a, this point will have a high concentration of positive charges due to the electronegativity of the propellant.

Such electrostatic field intensification could encourage the aerosol droplets/particles from the edge of the plume to carry positive, rather than negative charges, hence partly offsetting the negative charge in the main plume emitted from the cone nozzle orifice, where overall net charge magnitude is reduced. Importantly, this process will depend on the polar component of the total surface energy and the relative capacity for each material to donate electrons to the evaporating HFA (with PTFE and Nylon having the lowest and highest γ^-, respectively).

Influence of Ethanol on Net Electrostatic Charge

When 1% w/w of ethanol co-solvent was added to HFA134a, a significant reduction of the negative net charge magnitude

Table II Surface Energy Parameters (mJ/m^2) for Each Actuator Block Material Determined Using Contact Angle Goniometry

Material	Dispersive energy	Total polar surface energy	Total surface energy
Nylon	40.8	27.6	68.3
PET	37.9	15.3	53.3
PE	37.6	13.7	51.4
PP	35.6	24.4	60.0
PTFE	21.0	1.6	22.6

was evident for all materials and both nozzle designs when compared with the ethanol free formulation (Student t-test, $p < 0.05$) (Fig. 5). In general a ~500 pC reduction in negative charge was observed.

As with the formulation containing HFA alone, no significant differences in net charge, between different materials, were found for the flat actuator geometry, when studying the formulation containing 1% w/w ethanol (One-way ANOVA, $p = 0.142$), apart for the PTFE material. A significant difference in net charge was found for the PTFE flat nozzle design where the net charged approached neutrality (–67.82 pC ± 67.3). For the cone nozzle design, the net charge of the 1% w/w ethanol formulation followed the same trend as for formulation containing HFA alone; however the magnitude was ~500 pC in favour of neutrality. Again, PP did not follow the reported triboelectric series but fitted the surface energy measurements with respect to polar surface energy and capacity for electron donation.

With an increase in co-solvent to 15% w/w ethanol (Fig. 6), a further, significant ($p < 0.005$) decrease in net charge was evident in aerosols generated from both nozzle designs. Net charges reached neutrality for all materials and reversed polarity in the case of PET and PTFE. Polyethylene and PTFE have the lowest polar charge component and it is likely this factor reduces the capacity for the ethanol/HFA mixture to scavenge and retain electrons as they are generated at the actuator block interface.

The reduction in charge when ethanol was added to HFA is likely due to an increased interaction (and consequently increased electron exchange) of the evaporating droplets with the material surface and change in conductivity and propensity for electron movement within the HFA/ethanol droplets. Specifically, the addition of ethanol reduces the evaporation rate of the propellant and increases the contact time between the droplets and the actuator material, therefore increasing the chance of electron exchange during such triboelectrification. Furthermore, the presence of ethanol could also alter the dielectric property of the formulation. Indeed, measurement of HFA/ethanol conductivity suggested this to be the case. Direct measurement of formulation conductivity indicated the resistance to decrease by ~2 orders of magnitude from $\sim 5 \times 10^{-8}$ mho/m for HFA alone, to 1×10^{-5} mho/m when 15% w/w HFA was added (53). This could be the result of both the ionisability of the ethanol molecule, which induces molecular interaction with the propellant reducing the HFA electron withdrawing nature. In addition, the evaporation rate for ethanol is relatively slower than the propellant, where ethanol is likely to form a thin coating on the actuator nozzle surfaces during the actuation process. It is possible that the solid surface will essentially be "masked" by an absorbed ethanol layer, hence changing the electrostatic potential and consequent charge exchange between surface modified by absorbed ethanol, and HFA 134a containing ethanol as co-solvent.

Influence of BDP on Net Electrostatic Charge

When BDP (0.1% w/w) was added into the formulation containing 15% w/w ethanol, a significant change in aerosol charging profile was observed for both cone geometry and material when compared with the HFA system containing 15% ethanol alone. The net charge for the BDP containing formulation, as a function of material and actuator block geometry, is shown in Fig. 7.

It is interesting to note that the magnitude of the charges observed when BDP was included in the formulation was greater than in the formulation containing 15% w/w ethanol alone. Such observation suggests the presence of BDP in low concentrations (0.1% w/w) 'dampens' the effect of high ethanol concentrations on reducing the charge to neutrality. BDP is a corticosteroid, with a relatively large molecule structure, compared with HFA 134a and ethanol and is capable of dipole-dipole and hydrogen bonding events giving rise to a complex electrostatic potential environment in the formulation. Additionally, it is important to recognise that the BDP is the only non-volatile component within the formulation. This will give rise to BDP enriched droplet surfaces during the evaporation process, altering charge profiles (54).

Consequently, contact between BDP and the actuator block surfaces are likely to be high as the volatile components start transitioning from liquid to gas phase, even as they pass into the pMDI sump and through the orifice geometry.

With respect to charge polarity, the flat nozzle design presented a negative net charge (from –316.83 pC ± 222.54 for Nylon to –442.07 pC ± 291.41 for Polypropylene, respectively), with the exception of PTFE (651.63 pC ± 160.61). In comparison, the net charge from aerosols generated in the cone geometry tended towards positivity, suggesting that interaction between the forming aerosol particles at this interface was governed by the interactions of the drying particles and material type across the increased surface area, as well as increased contact time between the propellant and the actuator surface of the cone.

In comparison with the HFA and HFA/ethanol mixtures there was not a direct relationship between the cone material and net charge; however, in general the data presented are in good agreement with previous studies using the ethanol-based Qvar™ formulation, which generates a positive net-charge when aerosolised from a polyethylene cone-geometry actuator, as in this study (12).

Relating the surface energy to the aerosol charge in the multi-component BDP-ethanol-HFA system is more complex than in simpler single and binary liquid systems, since there are three phases of matter involved. Furthermore, significant differences in net charge polarity when comparing the flat and cone geometries for aerosols generated from each material suggested that the generation of the particles at this interface were fundamentally different.

In general, the cone nozzle design for all materials resulted in a net charge with a reduced magnitude in comparison with the flat design. Triboelectrification is largely affected by the surface properties (55, 56) and for the cone nozzle design a larger surface area would result in more electron exchange between the actuator materials and the aerosol droplets in comparison with the flat nozzle, given more varied charging pattern which is reflected in the results. Additionally, the presence of sharp edges on the cone nozzle geometry could possibly lead to the release of electrons/ions of the opposite polarity due to local electrostatic field intensification. Interestingly, for the cone nozzle design all the homopolymers charged the resulting aerosol positively, suggesting that the BDP favours electron donation when exposed to the cone surface.

To further understand the influence of orifice material and geometry on aerosol generation it is important to evaluate the aerodynamic properties of each system.

Influence of Orifice Material and Geometry on the Aerodynamic Properties

Electrostatic charge measurements have indicated that the actuator orifice geometry and material can directly influence the charge generated on the aerosolised droplets. However, it is important to consider how charge affects the aerosol particle size distribution profile and mass of fine particles that potentially enter the respiratory tract. In order to do this the mass of BDP particles collected from all stages of the ELPI impactor, induction port and actuator block were analysed and aerodynamic parameters were derived.

Ex-valve (Total Dose) Analysis

Analysis of the ex-valve dose suggested no significant difference between actuator geometries or material used. Total recovered drug masses were 248.09 μg±23.49 and 237.53 μg±11.59 for BDP, from flat and cone geometries, respectively.

Aerosol Particle Size Distribution

Impactor plate derived cumulative percentage particle mass distributions for BDP aerosolised from flat and cone geometries are shown in Fig. 8. The mass median aerodynamic diameter (MMAD) were calculated assuming linearity between 84 and 16% of the cumulative mass undersize lognormal distribution, and the geometric standard deviation (GSD) was determined from $(d_{0.84}/d_{0.16})^{1/2}$. The cumulative undersize plots showed no significant differences between the different materials with the same nozzle geometry or between the two different nozzle designs. Mean MMAD values across all materials were 0.73 μm±0.01 and 0.76 μm±0.01 and GSD values 2.01±0.07 and 2.00±0.03 for flat and cone geometries, respectively. Such observations suggest that actuator geometry and material does not affect the particle size distribution generated from the pMDIs.

Aerosol Particle Mass Distribution

It is important to note that while the aerosol size distribution may be similar, irrespective of material or geometry, the number/mass of particles within the aerosol cloud may alter as a result of charge variation. To study this further, the fine particle mass (FPM) of particles ≤6.66 μm was calculated by summing stages 1–12 (size range 0.028–6.66 μm) of the ELPI. Additionally, the fine particle mass fraction (FPMF) was calculated based on the FPM as a function of the total ex-valve dose (TD) (Table III). The FPMF will be used as the representative figure of fine particles less than 5 μm that are considered as good inhalation aerosols for lung deposition.

Furthermore, the aerosol performance, expressed as Emitted Dose (ED), Fine Particle Dose (FPD, calculated assuming linearity of actual drug mass between 84 and 16% of the cumulative mass undersize lognormal distribution) and Fine Particle Fraction (FPF, as % of TD) are presented in Table III. Particle sizes less than 1 μm were defined as fine particles due the aerodynamic cut-off sizes of the ELPI impactor stages (Fig. 3) and corresponding deposition patterns for BDP pMDI in this study (e.g. >90% of the particles are less than 5 μm, Fig. 8, which is normally used as a representative size for fine particle in many aerosol studies). Statistical analyses of differences in FPF, FPD, ED, MMAD and GSD between materials and designs were carried out using both one-way ANOVA (unstacked) and Student *t*-test (heteroscedastic), where a p-value<0.05 was considered statistically significant.

As discussed before, the two mechanisms for electrostatic deposition are space charging and image force. For the former, a unipolar charged particle is more favorable to increase the deposition as particles repel each other (11). In this study, BDP pMDI aerosols have always resulted in a bipolar charge (Fig. 9), hence reducing the effect of space charging. As for the image charge, particle travelling within the free space of the airway wall create an electric field which cause dielectric changes on the wall surface and give rise to an image charge of opposite polarity that attract particles (11). This mechanism is greatly affected by the velocity of the particles, distance to the airway walls, humidity and the charges carried by the particles. These variables are carefully controlled under the test condition for this study, which reduced the effect of variation in image charging on particle deposition.

Further analysis using unstacked one-way ANOVA showed no difference in TD and ED for all materials and

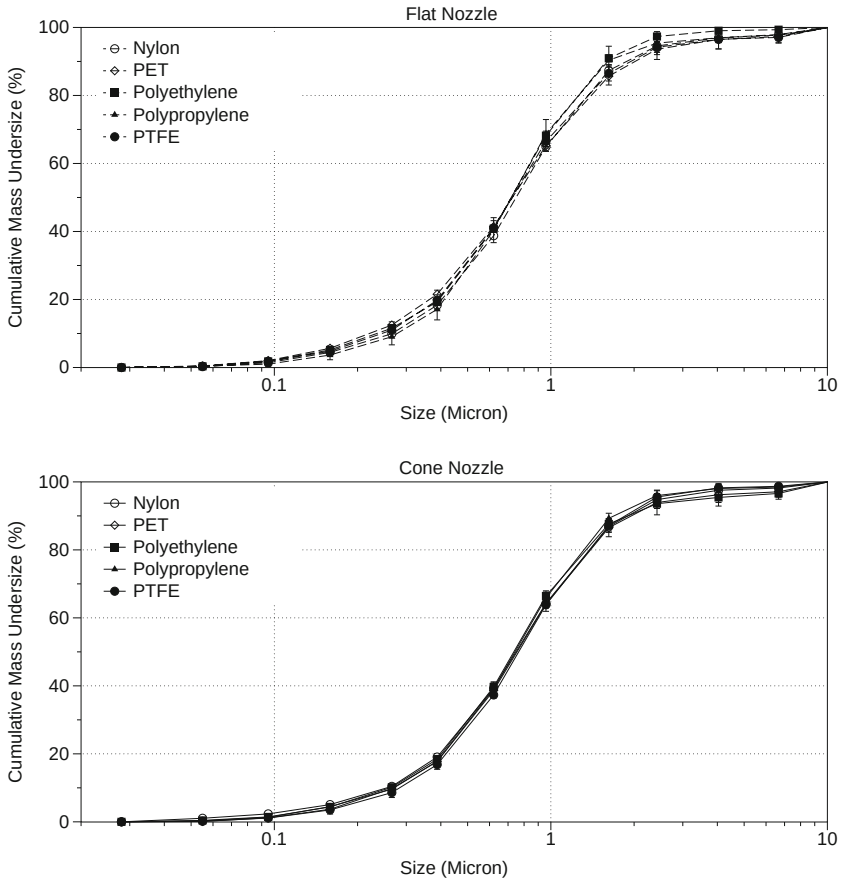

Fig. 8 Cumulative undersize plots for the 0.1% w/w BDP formulation containing 15% w/w ethanol and HFA with all materials and both nozzle designs in the ELPI, ($n = 3$, % ± SD)

Table III ED, FPD, FPF, MMAD and GSD Values for Formulation BDP in the ELPI, for Different Materials and Designs ($n = 3$, mean ± SD)

	Nylon	PET	Polyethylene	Polypropylene	PTFE
Flat Nozzle*					
TD (μg)	262.02 (±46.26)	263.78 (±66.37)	267.10 (±45.34)	234.31 (±30.11)	213.23 (±11.09)
ED (μg)	250.84 (±45.60)	250.97 (±62.71)	254.47 (±44.96)	225.73 (±30.36)	207.20 (±11.20)
FPM (μg≤6.66 μm)	91.37 (±14.78)	70.26 (±21.23)	126.92 (±28.48)	61.96 (±11.10)	55.10 (±6.09)
FPMF (μg≤6.66 μm)	34.97 (±2.23)	26.43 (±1.24)	47.25 (±2.47)	26.34 (±1.29)	25.83 (±2.29)
FPD (μg≤1 μm)	60.16 (±9.78)	46.43 (±13.64)	85.57 (±18.41)	41.42 (±6.01)	37.17 (±3.81)
FPF (%≤1 μm)	24.08 (±1.93)	18.38 (±0.74)	33.49 (±1.39)	18.34 (±0.74)	17.94 (±1.58)
MMAD (μm)	0.75 (±0.01)	0.74 (±0.02)	0.72 (±0.01)	0.74 (±0.04)	0.72 (±0.01)
GSD	2.01 (±0.06)	2.12 (±0.07)	1.94 (±0.01)	1.96 (±0.11)	2.03 (±0.08)
Cone Nozzle					
TD (μg)	236.23 (±28.95)	234.54 (±24.51)	235.78 (±29.44)	224.66 (±12.27)	256.44 (±40.99)
ED (μg)	230.70 (±20.05)	217.61 (±24.92)	221.32 (±28.19)	211.30 (±14.04)	241.31 (±36.63)
FPM (μg≤6.66 μm)	79.16 (±8.76)	72.93 (±7.32)	87.87 (±10.36)	87.29 (±15.20)	85.85 (±17.72)
FPMF (μg≤6.66 μm)	32.12 (±0.86)	31.11 (±0.28)	37.31 (±1.85)	38.79 (±5.81)	33.42 (±4.19)
FPD (μg≤1 μm)	51.31 (±4.92)	47.86 (±4.75)	59.01 (±6.63)	57.68 (±10.86)	54.79 (±10.16)
FPF (%≤1 μm)	22.23 (±0.24)	22.02 (±0.36)	26.72 (±1.60)	27.24 (±4.26)	22.66 (±2.10)
MMAD (μm)	0.76 (±0.02)	0.76 (±0.01)	0.74 (±0.01)	0.75 (±0.03)	0.77 (±0.01)
GSD	2.03 (±0.01)	2.03 (±0.06)	1.99 (±0.01)	1.95 (±0.01)	2.00 (±0.06)

*The results are average of three measurements. *TD* total Ex-valve dose; *ED* emitted dose; *FPM* fine particle mass ≤6.66 μm; *FPMF* fine particle mass fraction ≤6.66 μm; *FPD* fine particle dose≤1 μm; *FPF* fine particle fraction≤1 μm; *MMAD* mass median aerodynamic diameter; *GSD* geometric standard deviation

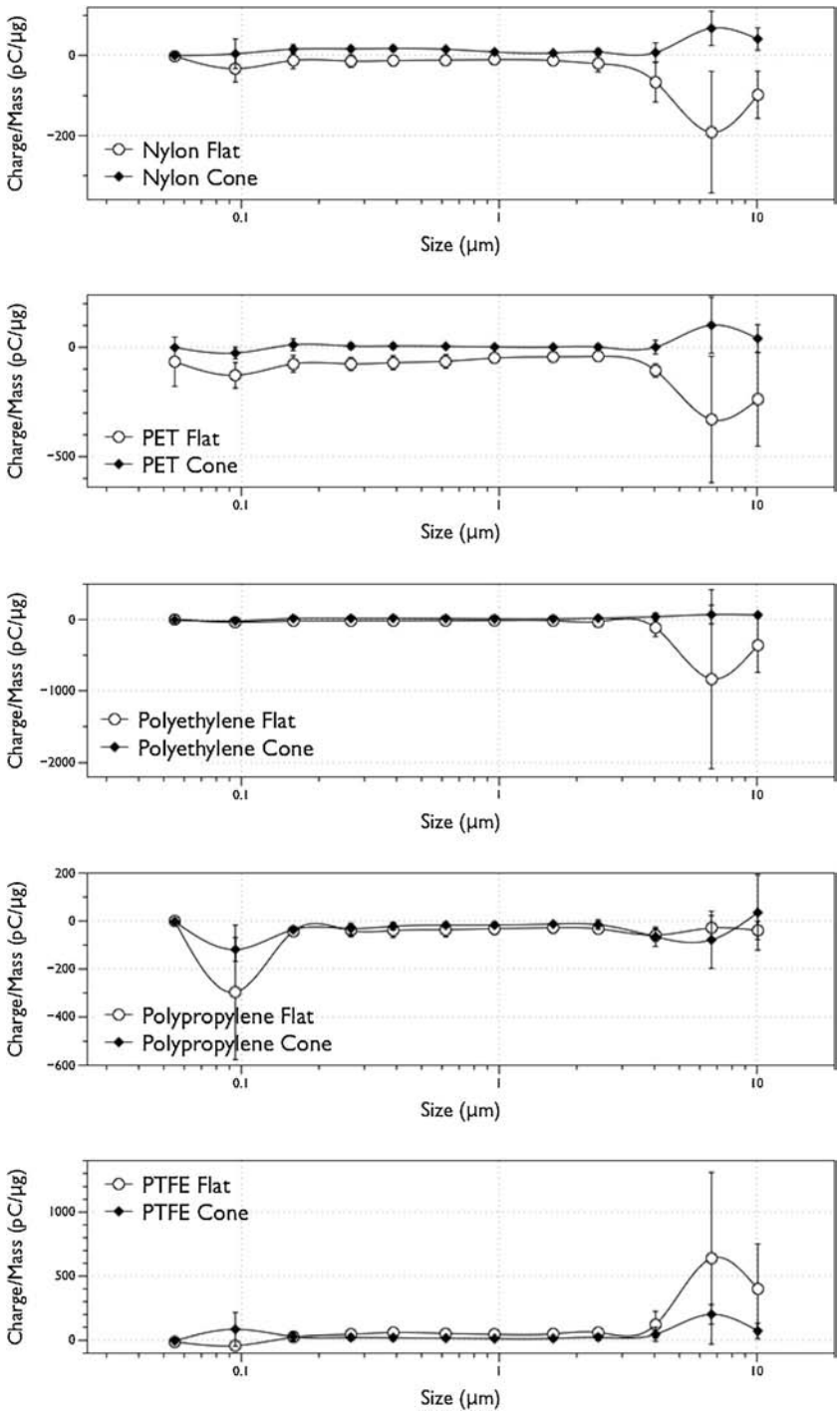

Fig. 9 Charge to mass ratio for the 0.1% w/w BDP formulation containing 15% w/w ethanol and HFA with all materials and both nozzle designs, ($n = 3$, pC/μg $\pm$ SD).

both nozzle designs. For the flat nozzle, significant differences across materials are observed for FPM, FPD, FPMF, FPF (one-way ANOVA, $p < 0.005$ for all, respectively), where for the cone orifice, only FPF is different with different actuator materials (one-way ANOVA, $p < 0.05$). Comparison between the performance parameters of the two nozzle designs, for the same materials (listed in Table III), show no significant differences, except for PE which demonstrates a difference in FPM and FPF between flat and cone orifice (Student *t*-test, heteroscedastic, $p < 0.05$). PET also showed a significantly higher FPMF with cone nozzle compared with flat (Student *t*-test, heteroscedastic, $p < 0.05$). At the same time, PE with the flat nozzle exhibits the highest FPM (126.92 µg $\pm$ 28.48) and the highest FPMF (47.25% $\pm$ 2.47) compared with other materials and nozzle designs. Such differences in aerosol performance with different actuator materials and nozzle designs could be potentially caused by the change in the charge homogeneity in the spray plume. The ELPI is only able to

give mean charge results, with no indication of the bipolar charge portion from the aerosols. It is hard to determine whether a certain size range has a dominant charge polarity or the specific amount of charge carried by a single particle. For example, if particles larger than (e.g. >5 μm) have a unipolar charge, it is very likely to cause higher throat deposition due to the repulsive force between particles with same polarity (space charge mechanism).

The Effect of Ethanol Concentrations and Nozzle Designs on the Charge-to-Mass Ratio of the BDP Solution pMDI Aerosol Performance

To extend the investigation of the relationship between particle size distribution and electrostatic charges, the mean net charge data were divided by mean mass obtained for the BDP formulation to produce charge-to-mass ratios (pC/μg) for each ELPI cut-off stage, thus obtaining the elementary charge distribution according to particle sizes. Analysis of the charge/mass (pC/μg) ratio across all twelve stages of the ELPI for all five materials and nozzle designs is presented in Fig. 9.

Comparing cone and flat nozzles, significant differences in charge to mass ratio for particle sizes in the range between 0.266 and 2.42 μm (unstacked one-way ANOVA analysis, $p < 0.005$) were observed for all five materials. Large variations in pC/μg were observed for particle sizes greater than 2.42 μm and smaller than 0.266 μm (for all materials and both nozzle design) (Fig. 9). The former could be a result of the evaporation process; the BDP formulation contains ethanol at 15% w/w, which reduces the evaporation rate of HFA 134a. This results in large un-evaporated droplets that impact on the top stages of the ELPI, causing the electrostatic charge measurements to vary to a higher degree.

For Nylon, PET and PE with the flat nozzle design, an increase in the negative charge associated with the aerosol is evident. For PP this is reduced towards neutrality, and for PTFE the charge magnitude is significantly increased but towards positive polarity (Fig. 8). For the cone nozzle, charges between all materials are also significantly different (one-way ANOVA, $p < 0.05$), but with a tendency to neutrality, indicative of either an increased electron exchange with the larger cone surface area or possible electron discharge due to accumulated charges on the surface of the cone nozzle that can consequently neutralise the charges carried by the aerosol.

An interesting observation is that the pC/μg standard deviations for the lowest impactor stages, particles/droplets with a size below 0.266 μm, are also very large. Since the lower stages contain very small BDP mass values, the charge to mass division results in large and variable q/m results. However, even taking these errors into account, the pC/μg values are very high, likely due to the high specific surface area contributed by the very fine aerosol droplets constituted by the HFA propellant and ethanol.

CONCLUSIONS

This study has demonstrated that the electrostatic charging profiles arising from a solution pMDI formulation containing ethanol as co-solvent can be influenced significantly by the actuator material, nozzle design and formulation components. Significant differences in the net charge of pMDI formulations containing HFA134a propellant and two different ethanol concentrations (1 and 15% w/w), with and without BDP, demonstrated how the use of ethanol could influence the charge magnitude of the exiting aerosol after actuation. Furthermore, it was shown that BDP interactions with ethanol and HFA could have an influence on the electrostatic charge of the aerosol. Additionally, it was demonstrated how actuator nozzle design can influence the charging pattern of pMDI aerosols and by choosing different combination of actuator materials and orifice design, the fine particle fractions of the formulation could be altered. These results are invaluable in the formulation of high performance solution pMDI and highlight the importance such factors may have on therapeutic properties of pMDI formulations.

ACKNOWLEDGMENTS AND DISCLOSURES

This research was supported under Australian Research Council's Linkage Projects funding scheme (project number LP100200156). A/Professor Young is the recipient of an Australian Research Council Future Fellowship (project number FT110100996). A/Professor Traini is the recipient of an Australian Research Council Future Fellowship (project number FT12010063).

REFERENCES

1. Chan TL, Yu CP. Charge effects on particle deposition in the human tracheobronchial tree. Ann Occup Hyg. 1982;26(1-4):65–75.
2. Melandri C, Prodi V, Tarroni G, Formignani M, Bompane GF, Dezaiacomo T, *et al*. Deposition of unipolarly charged-particles in human respiratory-tract. Health Phys. 1977;33(3):273.
3. Tarroni G, Melandri C, Prodi V, Dezaiacomo T, Formignani M, Bassi P. An indication on the biological variability of aerosol total deposition in humans. Am Ind Hyg Assoc J. 1980;41(11):826–31.
4. Fraser DA. Deposition of unipolar charged particles in lungs of animals. Arch Environ Health. 1966;13(2):152–61.
5. Ferin J, Mercer TT, Leach LJ. The effect of aerosol charge on the deposition and clearance of TiO2 particles in rats. Environ Res. 1983;31(1):148–51.
6. Vincent JH, Johnston WB, Jones AD, Johnston AM. Static electrification of airborne asbestos—a study of its causes, assessment and effects on deposition in the lungs of rats. Am Ind Hyg Assoc J. 1981;42(10):711–21.
7. Ingham DB. Precipitation of charged-particles in human airways. J Aerosol Sci. 1981;12(2):131–5.
8. Yu CP, Chandra K. Precipitation of submicron charged-particles in human lung airways. B Math Biol. 1977;39(4):471–8.

9. Diu CK, Yu CP. Deposition from charged aerosol flows through a pipe bend. J Aerosol Sci. 1980;11(4):397–402.
10. Thiagarajan V, Yu CP. Sedimentation from charged aerosol flows in parallel-plate and cylindrical channels. J Aerosol Sci. 1979;10(4): 405–10.
11. Finlay WH. The mechanics of inhaled pharmaceutical aerosols: An introduction: Access Online via Elsevier; 2001
12. Kwok PCL, Chan HK. Electrostatics of pharmaceutical inhalation aerosols. J Pharm Pharmacol. 2009;61(12):1587–99.
13. Karner S, Urbanetz NA. The impact of electrostatic charge in pharmaceutical powders with specific focus on inhalation-powders. J Aerosol Sci. 2011;42(6):428–45.
14. Hao T, Tukianen J, Nivorozhkin A, Landrau N. Probing pharmaceutical powder blending uniformity with electrostatic charge measurements. Powder Technol. 2013
15. Pu Y, Mazumder M, Cooney C. Effects of electrostatic charging on pharmaceutical powder blending homogeneity. J Pharm Sci-Us. 2009;98(7):2412–21.
16. Šupuk E, Hassanpour A, Ahmadian H, Ghadiri M, Matsuyama T. Tribo-electrification and associated segregation of pharmaceutical bulk powders. KONA Powder and Particle Journal. 2011;29: 208–23.
17. Mitchell JP, Coppolo DP, Nagel MW. Electrostatics and inhaled medications: influence on delivery via pressurized metered-dose inhalers and add-on devices. Respir Care. 2007;52(3):283–300.
18. Kwok PCL, Trietsch SJ, Kumon M, Chan HK. Electrostatic charge characteristics of jet nebulized aerosols. J Aerosol Med Pulm D. 2010;23(3):149–59.
19. Hoe S, Traini D, Chan HK, Young PM. The influence of flow rate on the aerosol deposition profile and electrostatic charge of single and combination metered dose inhalers. Pharmaceut Res. 2009;26(12): 2639–46.
20. Kwok PCL, Glover W, Chan HK. Electrostatic charge characteristics of aerosols produced from metered dose inhalers. J Pharm Sci-Us. 2005;94(12):2789–99.
21. Adi H, Kwok PCL, Crapper J, Young PM, Traini D, Chan HK. Does electrostatic charge affect powder aerosolisation? J Pharm Sci-Us. 2010;99(5):2455–61.
22. Byron PR, Peart J, Staniforth JN. Aerosol electrostatics .1. Properties of fine powders before and after aerosolization by dry powder inhalers. Pharmaceut Res. 1997;14(6):698–705.
23. Hoe S, Young PM, Traini D. Dynamic electrostatic charge of lactose-salbutamol sulphate powder blends dispersed from a cyclohaler (R). Drug Dev Ind Pharm. 2011;37(11):1365–75.
24. Hoe S, Traini D, Chan HK, Young PM. The contribution of different formulation components on the aerosol charge in carrier-based dry powder inhaler systems. Pharmaceut Res. 2010;27(7): 1325–36.
25. Kwok PCL, Chan HK. Effect of relative humidity on the electrostatic charge properties of dry powder inhaler aerosols. Pharmaceut Res. 2008;25(2):277–88.
26. Ali M, Mazumder MK, Martonen TB. Measurements of electrodynamic effects on the deposition of MDI and DPI aerosols in a replica cast of human oral-pharyngeal-laryngeal airways. J Aerosol Med Pulm D. 2009;22(1):35–44.
27. Newman SP. Principles of metered-dose inhaler design. Respir Care. 2005;50(9):1177–90.
28. Dunbar C. Atomisation mechanisms of the pressurized metered dose inhaler. Part Sci Technol. 1997;15(3–4):253–71.
29. Wiener M. How to formulate aerosols to obtain the desired spray pattern. J Soc Cosmet Chem. 1958;9:289–97.
30. Clark AR. MDIs: physics of aerosol formation. Journal of Aerosol Medicine. 1996;9(s1):S-19–26.
31. Newman S, Clarke S. Therapeutic aerosols 1–physical and practical considerations. Thorax. 1983;38(12):881–6.
32. Usmani OS, Biddiscombe MF, Barnes PJ. Regional lung deposition and bronchodilator response as a function of β2-agonist particle size. American journal of respiratory and critical care medicine. 2005;172(12):1497–504.
33. Dhand R, Malik S, Balakrishnan M, Verma S. High speed photographic analysis of aerosols produced by metered dose inhalers. J Pharm Pharmacol. 1988;40(6):429–30.
34. Newman SP. Aerosol deposition considerations in inhalation therapy. CHEST Journal. 1985;88(2):152S–60S.
35. Smyth HDC. The influence of formulation variables on the performance of alternative propellant-driven metered dose inhalers. Adv Drug Deliver Rev. 2003;55(7):807–28.
36. Wildhaber JH, Devadason SG, Eber E, Hayden M, Everard M, Summers Q, *et al*. Effect of electrostatic charge, flow, delay and multiple actuations on the in vitro delivery of salbutamol from different small volume spacers for infants. Thorax. 1996;51(10): 985–8.
37. Kwok PCL, Collins R, Chan HK. Effect of spacers on the electrostatic charge properties of metered dose inhaler aerosols. J Aerosol Sci. 2006;37(12):1671–82.
38. Anhoj J, Bisgaard H, Lipworth BJ. Effect of electrostatic charge in plastic spacers on the lung delivery of HFA-salbutamol in children. Brit J Clin Pharmaco. 1999;47(3):333–6.
39. Kwok PCL, Noakes T, Chan HK. Effect of moisture on the electrostatic charge properties of metered dose inhaler aerosols. J Aerosol Sci. 2008;39(3):211–26.
40. Berry J, Heimbecher S, Hart JL, Sequeira J. Influence of the metering chamber volume and actuator design on the aerodynamic particle size of a metered dose inhaler. Drug Dev Ind Pharm. 2003;29(8):865–76.
41. Smyth H, Brace G, Barbour T, Gallion J, Grove J, Hickey AJ. Spray pattern analysis for metered dose inhalers: effect of actuator design. Pharmaceut Res. 2006;23(7):1591–6.
42. Smyth H, Hickey AJ, Brace G, Barbour T, Gallion J, Grove J. Spray pattern analysis for metered dose inhalers I: orifice size, particle size, and droplet motion correlations. Drug Dev Ind Pharm. 2006;32(9): 1033–41.
43. Carter P, Rowley G, Roughley N, Suggett J. Electrostatic charge accumulation and decay in pharmaceutical polymer materials used in metered dose inhalers. J Pharm Pharmacol. 1998;50:55.
44. Bailey AG. Electrostatic phenomena during powder handling. Powder Technol. 1984;37:71–85.
45. Gallo CF, Lama WL. Classical electrostatic description of work function and ionization-energy of insulators. IEEE T Ind Appl. 1976;12(1):7–11.
46. Ndama AT, Guigon P, Saleh K. A reproducible test to characterise the triboelectric charging of powders during their pneumatic transport. J Electrostat. 2011;69(3):146–56.
47. Saleh K, Ndama AT, Guigon P. Relevant parameters involved in tribocharging of powders during dilute phase pneumatic transport. Chem Eng Res Des. 2011;89(12A):2582–97.
48. Bailey AG. Charging of solids and powders. J Electrostat. 1993;30: 167–80.
49. Lacks DJ, Levandovsky A. Effect of particle size distribution on the polarity of triboelectric charging in granular insulator systems. J Electrostat. 2007;65(2):107–12.
50. Good RJ. Contact-angle, adhesion and wetting—a critical-review. Abstr Pap Am Chem S. 1992;203:2-COLL.
51. Girifalco LA, Good RJ, Balestic P, Magat M, Leftin HP, Hall WK, *et al*. A theory for estimation of surface and interfacial energies. 1. Derivation and application to interfacial tension (vol 61, pg 904, 1957). J Phys Chem-Us. 1960;64(12):1960.

52. Adamson A. Physical chemistry of surfaces. 4th ed. New York: Wiley-Interscience; 1982.
53. Lewis D. Determination of electrical parameters of some propellants. Personal email communication to the author May 2012.
54. Zhu B, Traini D, Chan HK, Young P. The Effect of Ethanol on the Formation and Physico-chemical Properties of Particles Generated from Solution-based Pressurized Metered Dose Inhalers. Drug Dev Ind Pharm. 2013.
55. Allen RC. Triboelectric generation: getting charged. Ee-Eval Eng. 2000;39(11):S4.
56. Akbulut M, Alig ARG, Israelachvili J. Triboelectrification between smooth metal surfaces coated with self-assembled monolayers (SAMs). J Phys Chem B. 2006;110(44):22271–8.